Journal of Alzheimer's Disease 23 (2011) 195–206
DOI 10.3233/JAD-2010-100966
IOS Press

Enhanced Expression of the Voltage-Dependent Anion Channel 1 (VDAC1) in Alzheimer's Disease Transgenic Mice: An Insight into the Pathogenic Effects of Amyloid-β

Mar Cuadrado-Tejedor[a,c,d,1], Marcos Vilariño[a,1], Felipe Cabodevilla[a], Joaquín Del Río[a,d], Diana Frechilla[a,d] and Alberto Pérez-Mediavilla[a,b,d,*]
[a]*Division of Neurosciences, CIMA, University of Navarra, Pamplona, Spain*
[b]*Department of Biochemistry and Molecular Biology, University of Navarra, Pamplona, Spain*
[c]*Department of Anatomy, University of Navarra, Pamplona, Spain*
[d]*Networking Research Center on Neurodegenerative Diseases, CIBERNED, Spain*

Accepted 16 September 2010

Abstract. The mitochondrial voltage-dependent anion channel 1 (VDAC1) is involved in the release of apoptotic proteins with possible relevance in Alzheimer's disease (AD) neuropathology. Through proteomic analysis followed by Western blotting and immunohistochemical techniques, we have found that VDAC1 is overexpressed in the hippocampus from amyloidogenic AD transgenic mice models. VDAC1 was also overexpressed in postmortem brain tissue from AD patients at an advanced stage of the disease. Interestingly, amyloid-β (Aβ) soluble oligomers were able to induce upregulation of VDAC1 in a human neuroblastoma cell line, further supporting a correlation between Aβ levels and VDAC1 expression. In hippocampal extracts from transgenic mice, a significant increase was observed in the levels of VDAC1 phosphorylated at an epitope that is susceptible to phosphorylation by glycogen synthase kinase-3β, whose activity was also increased. The levels of hexokinase I (HXKI), which interacts with VDAC1 and affects its function, were decreased in mitochondrial samples from AD models. Since phospho-VDAC and reduced HXKI levels favors a VDAC1 conformational state more prone to the release proapoptotic factors, regulation of the function of this channel may be a promising therapeutic approach to combat AD.

Keywords: Alzheimer's disease, amyloid-β, hexokinase I, phospho-VDAC1, voltage-dependent anion channel 1 (VDAC1)

INTRODUCTION

Alzheimer's disease (AD), the main cause of dementia among the aged people, is characterized by several neuropathological hallmarks, such as amyloid-β peptide (Aβ) enriched extracellular plaques, hyperphosphorylated tau-containing intracellular neurofibrillary tangles (NFT), and substantial loss of synapses and neurons [1]. Although the exact cause of AD is unknown, multiple lines of evidence implicate Aβ as the agent initiating the cascade of pathological events in all cases of AD [2]. The mutations in three genes [amyloid β-protein precursor (AβPP) and presenilins 1 and 2] linked to familial forms of the disease (fAD) have been shown to increase the production and/or deposition of Aβ in the brain (reviewed in [3]). On this basis, transgenic mice overexpressing mutant

[1] These authors contribute equally to this work.

*Correspondence to: Pérez-Mediavilla Alberto, Division of Neurosciences, CIMA, University of Navarra, Avda. de Pio XII 55, 31080 Pamplona, Spain. Tel.: +34 948 194700; Fax: +34 948 194715; E-mail: lamediav@unav.es.

ISSN 1387-2877/11/$27.50

genes linked to fAD are the most used animal models to study AD. These transgenic mice exhibit a range of AD-like molecular and cognitive alterations, including deficits in learning and memory, amyloid deposits, and gliosis (reviewed in [4]). The Tg2576 mouse expressing the human Swedish mutation is one of the best characterized lines of AβPP transgenic animals [5–7]. In this mouse, exponential accumulation of Aβ peptide in the brain starts between 7 and 12 months of age, and amyloid deposits and impaired memory in the water maze test appear at the age of 9–11 months [6, 8, 9].

Several studies have demonstrated a direct deleterious effect of Aβ on mitochondrial structure and function (reviewed in [10]). Addition of Aβ to mouse brain mitochondria induces cytochrome c release and mitochondrial swelling. Furthermore, Aβ accumulates in mitochondria in AD affected neurons and disturbs the balance of fission/fusion and mitochondrial movement dynamics [11, 12].

Voltage-dependent anion channel 1 (VDAC1), a major constituent of the outer mitochondrial membrane, is part of the mitochondrial permeability transition pore (MPTP) forming in the outer mitochondrial membrane a voltage-gated pore, which is important for passive diffusion of substances through the membrane. Three isoforms of VDAC (VDAC 1–3) have been found in humans and in different animal species [13]. Significantly, it has been shown that VDAC1 can assume a configuration that promotes the release of proapoptotic factors, such as cytochrome c [14]. Mitochondrial VDAC-inmunoreactive structures consistent with mitochondrial accumulation occurs in the dystrophic neurites of Aβ plaques in AD [15].

On this basis, and given the relationship between Aβ and mitochondrial dysfunction, we decided to analyze the amount and the activity of VDAC1 in Tg2576 mice at different ages. An increase in VDAC1 protein in mice with high levels of Aβ was detected. Augmented levels of VDAC1 were also found in postmortem brain tissue from AD patients at an advanced stage of the disease. Addition of Aβ soluble oligomers to SH-SY5Y cell cultures also led to increased levels of total VDAC1 suggesting a role of Aβ peptide in VDAC1 increase and phosphorylation which could facilitate the leakage of mitochondrial proapoptotic molecules.

MATERIALS AND METHODS

Animals

The Tg2576 line express the human 695-aa isoform of AβPP containing the Swedish double mutation (hAβPPSwe) [(AβPP695) Lys670-Asn, Met671-Leu] driven by the hamster prion promoter. In this line, the Aβ-peptide content in the brain accumulates exponentially between 7 and 12 months of age [6].

Line J20 produces the human 770-aa AβPP carrying the Swedish and Indiana (Val717Phe) fAD mutations under control of the platelet-derived growth factor (PDGF) promoter. In this mice levels of Aβ are significantly increased by the age of 4 months [16]. In all cases, results were compared with those obtained in non-transgenic littermates.

Mice were housed in a temperature-controlled room under a 12 h light/dark cycle with free access to food and water. Animal experimentation received the approval from the Ethical Committee of the University of Navarra, and was performed in accordance with the European Council Directive 86/609/CEE on Protection of Animals Used for Experimental and Other Scientific Purposes.

2D-electrophoresis

Iso-electric focusing (IEF) dimension

For IEF, samples of 800 μg of proteins were solubilized in 300 μl of rehydration solution [9.5 M urea, 4% (w/v) CHAPS, 1% (w/v) dithiothreitol, 0.5% Bio-Lyte 3–10 and bromophenol blue]. This mixture of sample-containing rehydration solution was applied in the strip holder channel. The solubilized proteins were loaded onto an immobilized linear pH gradient (IPG) strip, pH 5–8, 17 cm (Bio-Rad, CA, USA). Therefore, the IPG strips were lowered, gel side down, onto the rehydration solution, and overlayered with mineral oil. Iso-electric focusing was performed on a Protean IEF Cell (Bio-Rad, CA, USA) at 20°C as follows: 12–16 h at 50 V, 1 h at 200 V, 1 h at 500 V, 1 h at 1000 V, 30 min at 1000–8000 V, and 7 h at 8000 V. The strips were focused for a total of 60,000 V h. After IEF, the strips were equilibrated for two intervals of 5 min in equilibration buffer containing 6 M urea, 0.375 M Tris–HCl, 2% SDS, and 20% glycerol, pH 8.8. For the first equilibration step, we added dithiothreitol (2% w/v) to reduce the proteins. Thereafter the proteins were carbamidomethylated with 2.5% (w/v) iodoacetamide.

Second dimension electrophoresis

SDS–PAGE was performed on a vertical electrophoresis system. The equilibrated IPG strip was placed on top of a SDS-polyacrylamide gel (12.5% T; 2.6% C) (Bio-Rad, CA, USA) and sealed with low melting point agarose. Electrophoresis was carried out

at 20°C on a Protean xi Cell (Bio-Rad, CA, USA) using a two-phase program. The first phase was set at 85 V for 12 h and the second phase was set at 300 V for 1 h.

The proteins of the 2D-gels obtained were detected using a colloidal Coomassie G-250 staining (Bio-Rad, CA, USA). The stained gels were digitized with a GS-800 calibrated densitometer (Bio-Rad, CA, USA) and analyzed with the Discovery Series PDQuest 2-D software (Bio-Rad, CA, USA). Qualitative and quantitative differences were detected and only the spots of which the integrated intensity differed by a factor of 1.5 minimum and occurring on all gels were accepted.

Identification of proteins by mass spectrometry

The identification of proteins was realized at the proteomics unit of the Center for Applied Medical Research (CIMA) under the direction of Dr. Fernando J. Corrales. Gel spots corresponding to proteins differentially expressed were collected manually and processed on a MassPrep station from Micromass (Manchester, UK). Gel specimens were de-stained with 50 mM ammonium bicarbonate/50% (vol/vol) acetonitrile. Then, proteins were reduced with 10 mM DTT in 100 mM ammonium bicarbonate and alkylated with 55 mM iodoacetamide in the same buffer. In-gel protein digestion was performed with 6 ng/μl trypsin in 50 mM ammonium bicarbonate for 5 h at 37°C. The resulting peptides were extracted with 1% (vol/vol) formic acid/2% (vol/vol) acetonitrile. Finally, 2 μl samples were mixed with 2 μl of a saturated solution of α-cyano-4-hydroxy-*trans*cinnamic acid in trifluoroacetic acid 0.1%/50% (vol/vol) acetonitrile and spotted into a matrix-assisted laser desorption ionization (MALDI) target plate. Tryptic peptides were then analyzed on a MALDI-time-of-flight (TOF) GL-REF mass spectrometer (Micromass, Manchester, UK). Data processing was performed with MASSLYNX. Database searching (Swiss-Prot, TrEMBL, Ensembl) to identify proteins of interest from their peptide fingerprint, was performed with PROTEINLYNX GLOBAL SERVER (Micromass, Manchester, UK).

Preparation of Amyloid-β-Derived Diffusible Ligands (ADDLs)

ADDLs were prepared with synthetic $A\beta_{1\text{-}42}$ (Bachem, CA, USA) according to the procedure described previously [17]. In brief, the peptide was dissolved in 1,1,1,3,3,3,-hexafluoro-2-propanol (HFP) to 1 mM and incubated for 1 h at room temperature and 5 min on ice. The peptide was stored as a dried film at –80°C after evaporation of the HFP. The day before use, dried peptide was resuspended in DMSO anhydrous to a final concentration of 5 mM, sonicated for 10 min, and diluted with ice-cooled phenol red-free Ham's F-12 (Invitrogen, CA, USA) to 100 μM and placed at °C for 24 h to form ADDLs. Before adding to cells, oligomers solution was centrifuged at $14000 \times g$ for 10 min and the supernatant was used. An aliquot of this preparation was analyzed qualitatively by Western blotting (Fig. 5A).

SH-SY5Y cell cultures

The SH-SY5Y cell line was obtained from ATCC (CRL-2266) [18]. The cells were grown up to 90% confluence at 37°C and 5% CO_2 atmosphere in Dulbecco's modified Eagle's medium (DMEM)/F12 (Gibco, Invitrogen, CA, USA) supplemented with 10% fetal bovine serum (FBS) on 60 mm plates (Corning, MA, USA). Before treatment ADDL solution was dissolved up to a 5 μM in DMEM/F12 without FBS and added to cells for the indicated times.

Human AD samples and controls

A total of 9 individuals from the Thomas Willis Oxford Brain Collection were included in the study, 5 patients with clinical diagnosis of dementia, and 4 elderly normal controls. Those patients with dementia were an autopsied subset of subjects included in a prospective study of behavioral changes in clinically diagnosed as demented patients [19]. Diagnoses were made using Cambridge Mental Disorders of the Elderly Examination (CAMDEX) [20], DMS-III-R criteria [21], and NINCDS-ADRA criteria [22]. Cognitive status was assessed using the Mini-Mental State Examination (MMSE) [23]. All tissues from control patients were examined by a pathologist and were confirmed to be free of gross neuropathology; clinical information indicated no gross neurological or psychiatric disorder.

For all subjects, informed consent had been obtained from relatives before the removal of brain tissue at death and subsequent use of the material for research. The study had Local Ethics Committee's approval. At autopsy, brains were removed and blocks corresponding to frontal (Brodmann area 10, BA10) cortex were stored at –80°C until processing. All patients were found to meet CERAD criteria [24] for a diagnosis of AD, and all brains were Braak stage V or VI as assessed by a neuropathologist.

Production of protein extracts

Mice were killed by cervical dislocation and hippocampi were quickly dissected from the brains. Total tissue homogenates were obtained by homogenizing the hippocampus in ice-cold RIPA buffer [50 mM Tris–HCl pH 7.4, 0.25% sodium deoxicolate, 1% Nonidet P-40 (Roche Diagnostics, Mannheim, Germany), 150 mM NaCl, 1 mM EDTA, protease inhibitors (Complete^{TM} Protease inhibitor cocktail, Roche Diagnostics, Mannheim, Germany), and phosphatase inhibitors (1 mM Na_3VO_4, 1 mM NaF)]. The homogenates were sonicated for 10 s, incubated on ice 30 min and centrifuged at $19000 \times g$ for 20 min at 4°C. Protein concentration was determined (Bradford protein assay, Bio-Rad, CA, USA) and aliquots were stored at –80°C until used. To obtain protein homogenates from SH-SY5Y, cells were lysed in 100 μl of RIPA buffer and the same protocol as was followed.

Western blotting

For Western blot analysis, samples were mixed with an equal volume of 2X Laemmli sample buffer, resolved onto SDS-polyacrylamide gels and transferred to nitrocellulose membrane (Hybond ECL, Amersham Biosciences, UK). The membranes were blocked with 5% milk, 0.05% Tween-20 in PBS or TBS followed by overnight incubation with the following primary antibodies: goat polyclonal anti-VDAC1 [for mouse samples (1 : 200, Santa Cruz Biotechnology, Inc., CA, USA)], Anti-VDAC1 Rabbit pAb [for human samples (1/1000, Calbiochem, Merck Chemicals Ltd., Nottingham, UK)], rabbit polyclonal anti-phospho-glycogen synthase kinase-3β (GSK3β) Ser9 (1 : 000, Cell Signalling Technology, MA, USA), rabbit polyclonal anti-GSK3β (1 : 000, Santa Cruz Biotechnology, CA, USA), rabbit polyclonal anti-phospho-Akt Ser473 (1 : 1000, Cell Signalling Technology, MA, USA), goat polyclonal anti-Hexokinase I (1 : 500, Santa Cruz Biotechnology, CA, USA), rabbit polyclonal anti-phophothreonine (1 : 1000, Zymed laboratories, CA, USA), and goat polyclonal anti-Actin (1 : 10000, Santa Cruz Biotechnology, CA, USA).

For qualitative analysis of ADDL, an aliquot of the preparation were mixed with XT^{TM} sample buffer (Bio-Rad, CA, USA). Oligomers were separated in a Criterion^{TM} precast Bis-Tris 4–12% gradient (Bio-Rad, CA, USA) and transferred to a PVDF membrane with 0.2 μm removal rating (Hybond LFP, Amersham Biosciences, UK). The membranes were blocked with 5% milk, 0.05% Tween-20 in TBS followed by overnight incubation with the mouse monoclonal 6E10 antibody (1/1000, Chemicon, CA, USA).

In all cases, membranes were washed three times in PBS or TBS/Tween-20 and one wash in PBS or TBS alone, immunolabeled protein bands were detected by using HRP-conjugated anti-rabbit, anti-goat, or anti-mouse antibody (1 : 5000, Santa Cruz Biotechnology, CA, USA) following an enhanced chemiluminescence system (ECL, GE Healthcare Bioscience, UK), and autoradiographic exposure to Hyperfilm ECL (GE Healthcare Bioscience, UK). Signals quantification was performed using the Quantity OneTM software v.4.6.3 (Bio-Rad, CA, USA). When β-Actin or GSK3β where used as loading control, target and control antibodies where analyzed from the same blot after removing the antibody with stripping solution [Reblot Plus Strong (Millipore, MA, USA)].

Immunoprecipitation and mitochondrial fraction isolation

Immunoprecipitation was done according to the catch and release reversible immunoprecipitation system protocol (Upstate, NY, USA). Briefly, 100 μg of hipocampal homogenates were added to the antibody capture affinity ligand and the specific VDAC1 antibody and incubated in a catch and release spin column at room temperature for 1 h under continuous shaking. The column was then washed three times with the wash buffer (10% Nonidet P-40, 2.5% deoxycholic acid, 150 mM imidazole, pH 7.4). The immunoprecipitate was then eluted with Tris-based immunoprecipitation elution buffer and analyzed by Western blotting as above described.

For isolation of an enriched mitochondrial fraction from hippocampus, a mitochondria isolation kit (MITO-ISO1, Sigma, MO, USA) was used as recommended by the manufacturer.

Tissue processing for immunohistochemistry

Under xylazine/ketamine anesthesia, animals were perfused transcardially with saline and 4% paraformaldehyde in phosphate buffer (PB). After perfusion, brains were removed, post-fixed in the same fixative solution for 1 h at room temperature and cryoprotected in 30% sucrose solution in PB overnight at 4.0°C. Microtome sections (30 μm-thick) were cut coronally through the entire hippocampus, collected

free-floating and stored in 30% ethylene glycol, 30% glycerol, and 0.1 M PB at –20°C until processed.

Immunohistochemistry

Five free floating tissue sections comprising the hippocampal formation of three animals per group were processed for immunohistochemistry. Brain sections were washed (3 × 10 min) with phosphate buffer saline 0.125 M, pH 7.4 (PBS) and incubated in blocking solution (PBS containing 1% Triton X-100, 0.5% BSA) for 2 h at room temperature. Sections were incubated overnight at 4°C with the anti VDAC1 antibody (Santa Cruz Biotechnology Inc., CA, USA) diluted 1 : 1000 in blocking solution, washed with PBS, and incubated with the secondary antibody (Alexa Fluor 488 anti goat, Molecular Probes, OR, USA) diluted 1.200 in blocking solution. After washing with PBS (3 × 10 min), sections were rinsed in 0.5 μM To-Pro-3 (Invitrogen, OR, USA), air dried for 24 h, and cover-slipped with immu-mount (Thermo Scientific, PE, USA). To ensure comparable immunostaining, sections were processed together under identical conditions. For the assessment of non-specific primary immunostaining, some sections from each experimental group were incubated without the primary antibody; in this case no immunostaining was observed. Fluorescence signals were detected with confocal microscope LSM 510 Meta (Carl Zeiss, Germany); objective Plan-neofluar 20×/0.5. Images were captured at the level of maximum fluorescence.

Determination of Aβ levels

$A\beta_{42}$ levels were determined by using a sensitive sandwich ELISA kit from Biosource (Camarillo, CA, USA) following the protocol described in [25].

RESULTS

Identification of VDAC1 using a proteomics approach as an upregulated protein in the hippocampus of Tg2576 mice

Hippocampal proteins derived from 16-month-old Tg2576 or WT mice were separated by means of 2-D PAGE gels and analyzed on a MALDI-time-of-flight (TOF) GL-REF mass spectrometer. Data processing was performed with MASSLYNS. By quantitative and statistical analyses, a total of 87 visualized protein spots were differentially expressed between the two groups. These differentially expressed spots were then excised and subjected to in-gel tryptic digestion and identification by MALDI-TOF MS followed by peptide mass fingerprinting. Among the 87 differentially expressed proteins (not shown), VDAC1 (NCBI identification number: gi|10720404gi| and accession number: Q60932) was identified as that having the greatest magnitude of change, 4.3-fold increase in Tg2576 mice versus WT controls (Fig. 1).

Age-dependent increase of VDAC1 protein levels in the hippocampus of Tg2576 mice

VDAC1 protein levels were analyzed by western-blot in Tg2576 mice, which display significant Aβ production since 6–7 months and exhibit amyloid plaques at 10–12 months (Fig. 2C) [6, 8]. VDAC1 protein levels in extracts from hippocampus of 7 and 12-month-old Tg2576 mice were determined and compared with those in strain- and age-matched wild type N-Tg controls (Fig. 2A). In 7 month-old animals there was a significant increase in VDAC1, 25%, and in 12 month-old animals, this increase was much more marked, 98%, compared with N-Tg controls. VDAC1 levels were also analyzed in another amyloidogenic transgenic model of AD, J20 line, with brain overexpression of human AβPP harboring both Swedish and Indiana fAD mutations, and with marked Aβ brain accumulation by the age of 4 months (Fig. 2C) [16]. Seven month-old J20 mice displayed a significant elevation of VDAC1 in hippocampal homogenates (Fig. 2B) thus confirming that VDAC1 levels were increased in transgenic amyloidogenic models of AD. VDAC1 immunoreactivity in

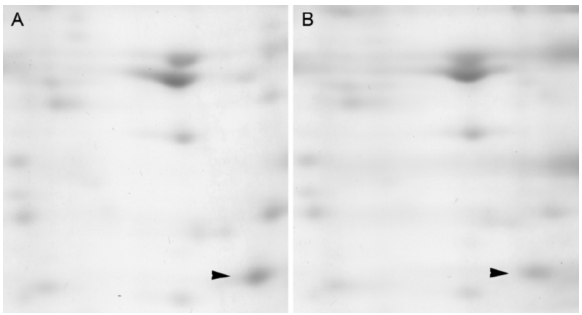

Fig. 1. Differential VDAC1 protein expression in the hippocampus of 16 month-old Tg2576 mice. Portion of a Coomassie-stained 2-D-gel from the hippocampus of Tg2576 (A) and non transgenic (B) age-matched mice. Quantitative intensity analysis of three independent experiments was performed to determine differential protein expression. Differentially expressed proteins were identified by MALDI-TOF MS followed by peptide mass fingerprinting. VDAC1 was increased by 4.3-fold ($p < 0.05$) related to non transgenic mice.

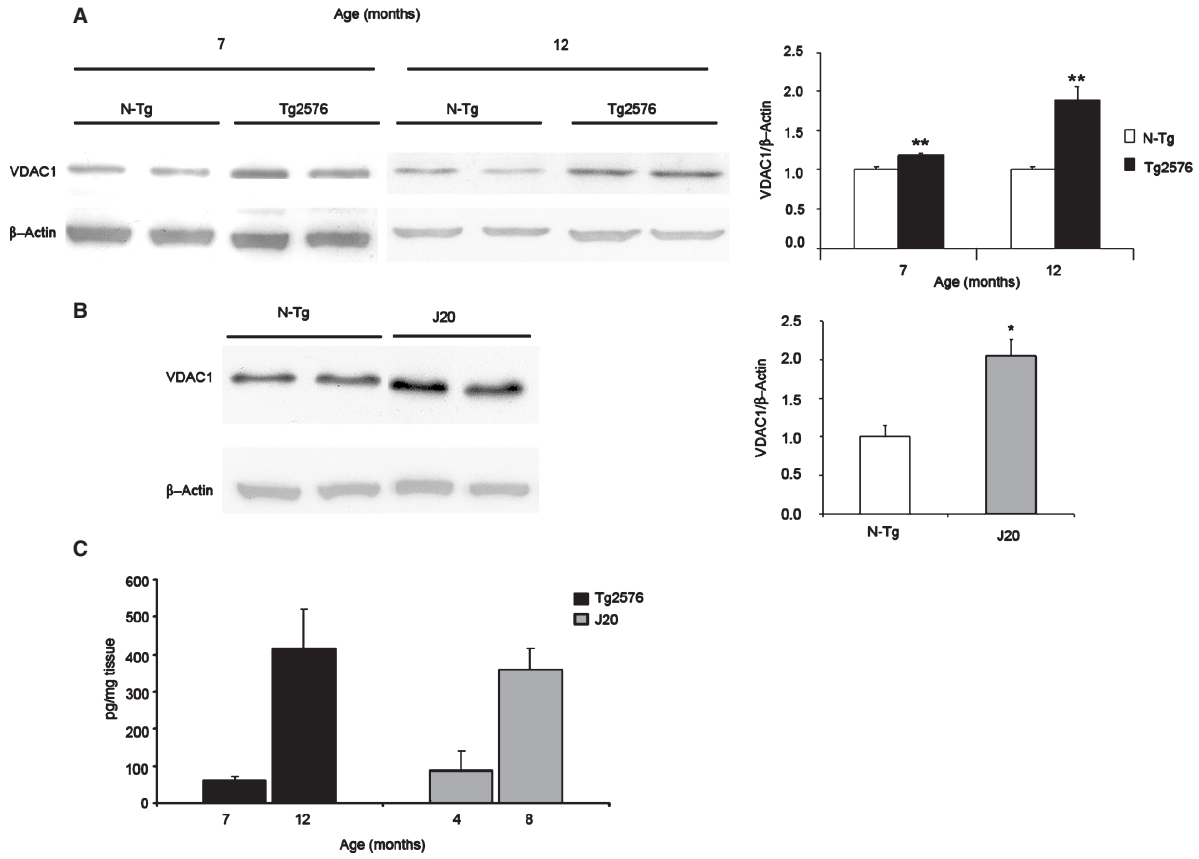

Fig. 2. VDAC1 levels in Tg2576 and J20 mice. Hippocampal homogenates from 7 month-old Tg2576 and J20 mice, 12 month-old Tg2576 mice, or age-matched control mice (N-Tg) were analyzed by Western blot. A) VDAC levels were significantly increased in 7 (25%) and 12 (98%) month old Tg2576 mice (**$p < 0.005$ vs. N-Tg, Student's t test). B) The J20 transgenic line also showed a 66% increase in VDAC levels (*$p < 0.05$ vs. N-Tg, Student's t test). C) Levels of $A\beta_{42}$ determined by ELISA. Bars represent the fold change of VDAC1/β-actin ratio (mean ± SEM) relative to N-Tg after the densitometric analysis of four different animals per group.

brain tissue was markedly increased in both amyloidogenic lines, primarily in the pyramidal cells in CA1 hippocampus subfield (Fig. 3) but also in the cerebral cortex (not shown). Interestingly, the expression of VDAC1 in the hippocampus of non transgenic animals was very scarce. Overall, the results provide convergent evidence of a strong correlation between high Aβ levels and increased levels of VDAC1.

Increase of VDAC1 in postmortem brain tissue from AD patients

The levels of VDAC1 were also determined in samples from human brain tissue. Due to the scarcity of hippocampal samples from AD patients, frontal cerebral cortex was used. It should be noted that, in AD, extracellular amyloid plaques first appear in the frontal cortex and not in the limbic system [26]. Brain tissue was obtained from five patients of AD (Braak stage V–VI) and from four control individuals with no history of neurological or psychiatric illness. A significant increase of VDAC1 protein was found in the frontal cortex of AD patients (Fig. 4). Despite marked interindividual differences, VDAC1 levels were significantly increased (55%) in AD patients related to non demented controls.

In vitro induction of VDAC1 protein expression by Aβ oligomers

Although the amyloid hypothesis states that central nervous system build-up of Aβ peptide is neurotoxic and triggers the pathological cascade [27], neurotoxicity of Aβ has been more recently attributed to its fibrillar forms referred to as ADDLs [28]. To check whether VDAC1 expression was affected by Aβ, SH-SY5Y neuroblastoma cells were incubated with 5 μM ADDLs and VDAC1 levels quantified in cell extracts

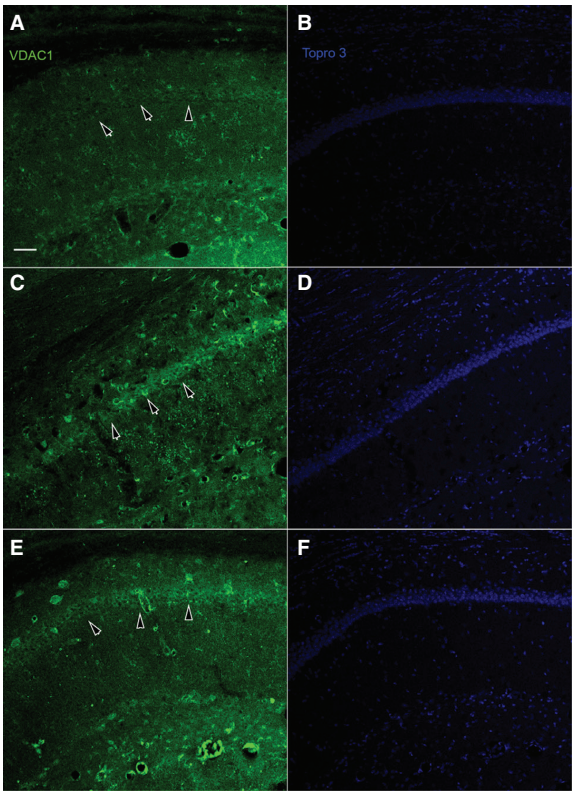

Fig. 3. VDAC1 immunoreactivity in hippocampal CA1 subfield. Representative confocal microscopy images of VDAC labeling in sections from 12 month-old non transgenic (A), Tg2576 (C) and 10 month-old J20 mice (E). Cell nuclei were labeled with Topro 3 (B, D, and F). As indicated by the arrows, CA1 can be easily identified by the VDAC immunostaining in both transgenic lines (C and E) whereas in non transgenic control CA1 is not defined by the VDAC immunoreactivity (A) ($n = 4$ animals per group, scale bar = 50 μm).

by Western blotting. As depicted on Fig. 5B, after 24 h of ADDLs incubation, cellular homogenates showed a significant increase in VDAC1 levels. A time course experiment revealed that as early as at 2 h and up to 24 h treatment with 5 μM ADDL led to a sustained increase in VDAC1 expression levels (Fig. 5C).

Enhanced VDAC1 phosphorylation and decreased hexoquinase in the hippocampus of Tg2576 mice

Activation of GSK3β disrupts the binding of HXK to mitochondria by phosphorylating VDAC1 and potentiates chemical-induced cytotoxicity [14]. To analyze its phosphorylation state, VDAC1 was immunoprecipitated from hippocampal extracts from 12 month-old Tg2576 or non transgenic age-matched mice, and immunoblotting was performed using a phosphothreonine-reactive antibody. As shown in

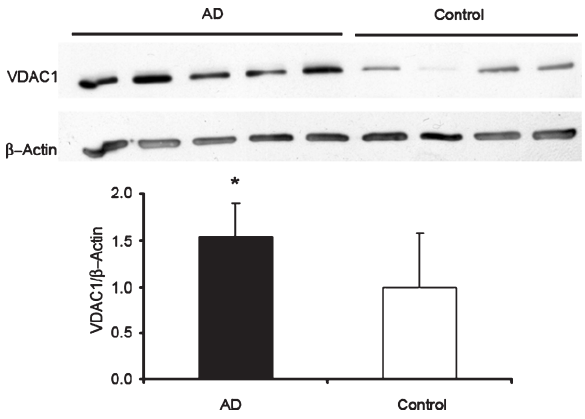

Fig. 4. VDAC1 protein levels quantified by Western blot in tissue lysates from the frontal cortex of AD patients (Braak stage V–VI, $n = 5$), and the corresponding non demented controls ($n = 4$). AD samples show a 1.6 fold change in VDAC levels ($^*p < 0.05$, Student's t test). Bars represent the fold change of VDAC1/β-actin ratio (mean ± SEM) relative to controls after the densitometric analysis of each individual determination.

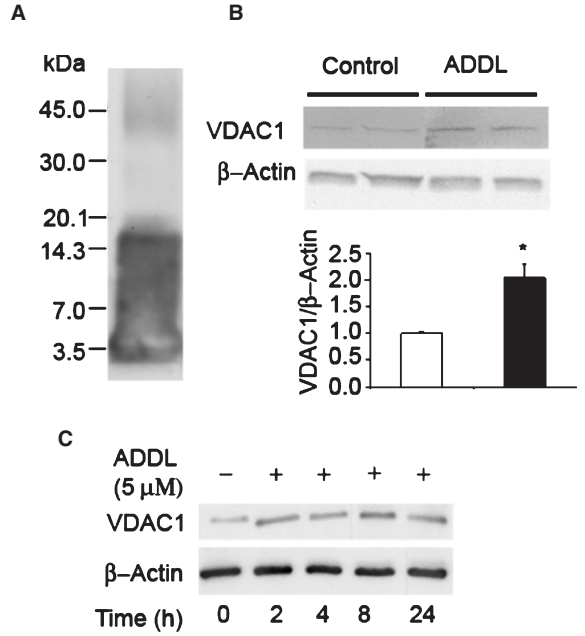

Fig. 5. ADDLs induce VDAC1 overexpresion in SH-SY5Y neuroblastoma cells. A) Western blot of ADDL preparation using 6E10 antibody (amino acids 1–17 of Aβ peptide). B) Cultures of SH-SY5Y neuroblastoma cells were incubated in presence of 5 μM ADDLs for 24 h. Bars represent the fold change of VDAC1/β-actin ratio (mean ± SEM) relative to control after the densitometric analysis of four different cell culture determinations ($^*p < 0.05$, Student's t test). C) Time course analysis of VDAC1 levels after incubation of SH-SY5Y neuroblastoma cells with 5 μM ADDL for the indicated period of time.

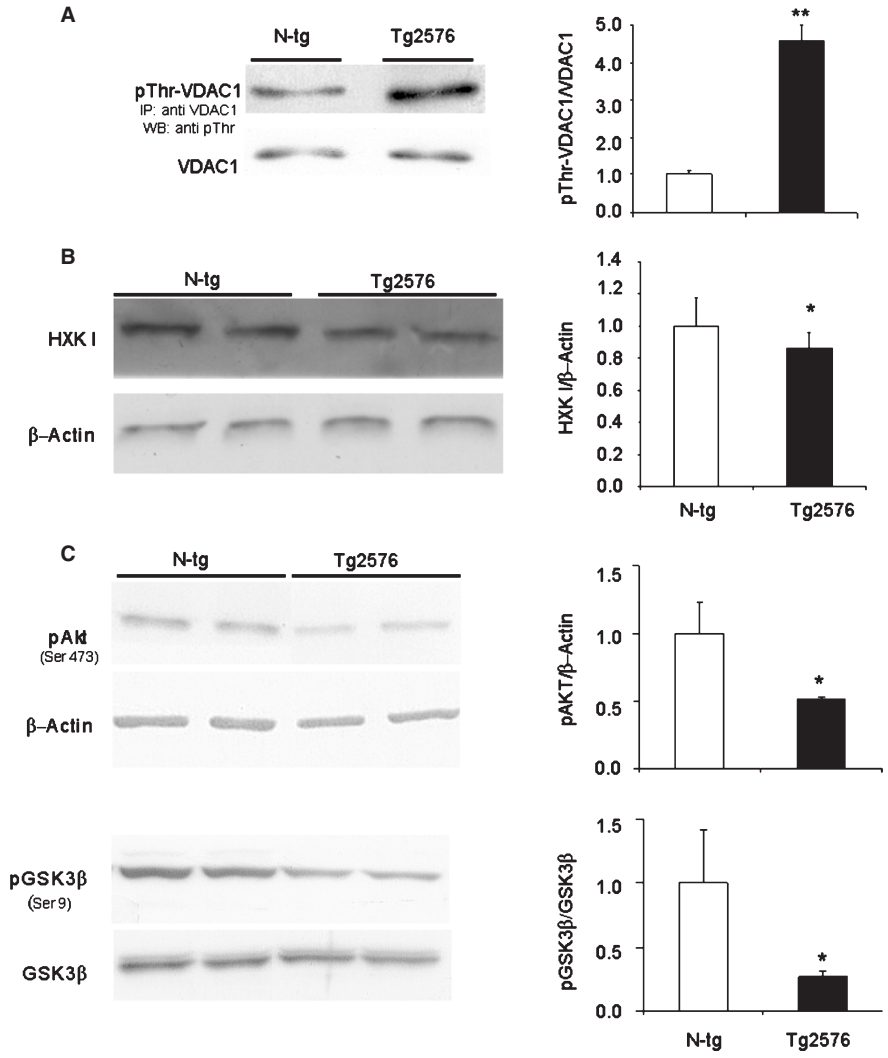

Fig. 6. Phosphothreonine-VDAC1 (phospho Thr-VDAC1) is increased in Tg 2576 and prevents the VDAC-HXK I interaction. A) Hippocampal homogenates were immunoprecipitated with anti-VDAC1 antibody and immunoprecipitates blotted and probed with an anti-phosphothreonine-reactive antibody or with an anti-VDAC1 antibody as a control of loading. Phosphorylated VDAC1 levels were significantly increased in Tg2576 related to non transgenic age matched controls (N-Tg) (**$p < 0.005$, Student's t test). B) Mitochondrial HXK I was determined by immunoblotting mitochondrial homogenates with anti-HXK I antibody. A significantly lower amount in mitochondrial HXKI was found in Tg2576 mice related to N-Tg (*$p < 0.05$, Student's t test). C) Hippocampal homogenates were blotted and incubated with anti-pAkt (Ser473, active form) and anti-pGSK3β (Ser9, inactive form) antibodies. β-Actin and total GSK3β were used as a control of charge for pAkt and pGSK3β respectively. Tg2576 mice showed a significant decrease in Akt activity (*$p < 0.05$, Student's t test) and an increase in GSK3β activity (*$p < 0.05$, Student's t test), one of the VDAC phosphorylating kinase. Bars represent the fold change of represented ratios (mean ± SEM) relative to N-Tg after the densitometric analysis of four different determinations.

Fig. 6A, there was a significant elevation in the levels of threonine-phosphorylated VDAC1 in samples from Tg2576 mice when compared with those from non transgenic mice. Phosphorylation of VDAC and the VDAC-HXK interaction are important factors for apoptosis. To determine if VDAC phosphorylation correlates with an altered balance of the VDAC : HXK ratio, mitochondrial HXK was determined and found to be significantly decreased in hippocampal extracts from Tg2576 animals (Fig. 6A).

Deactivation of Akt and activation of GSK3β in AD models

To investigate whether the Akt/GSK3β signaling pathway could be involved in the increase in VDAC1

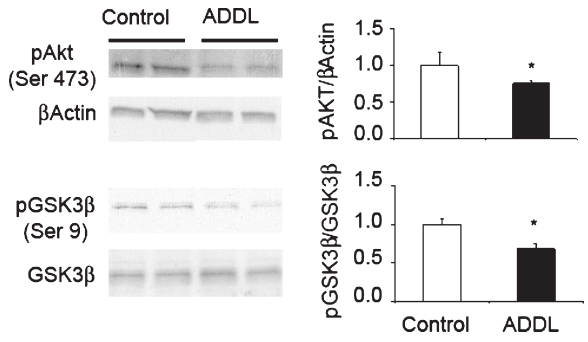

Fig. 7. $A\beta_{1-42}$ oligomers (ADDL) induce Akt inhibition and GSK3β activation in SH-SY5Y neuroblastoma cells. Cultures of SH-SY5Y neuroblastoma cells were incubated in presence of 5 μM ADDLs for 24 h. ADDL treated cells showed a significant decrease in active Akt (pAKT-Ser473) ($*p < 0.05$, Student's t test) and an increase in active GSK3β (pGSK3β-Ser9) ($*p < 0.05$, Student's t test). Bars represent the fold change of represented ratios (mean ± SEM) relative to non treated cells (control) after the densitometric analysis of four different determinations.

phosphorylation shown in the hippocampus of Tg2576 mice, we analyzed the levels of pSer473-Akt (active form) and pSer9-GSK3β (inactive form). VDAC1 has an epitope that may be phosphorylated by GSK3β [14]. Compared with control mice, Tg2576 mice showed a significant decline in pAkt levels averaging 49%, and a concomitant decline, 73%, in the levels of the inactive GSK3β form (Fig. 6B). To test whether ADDLs addition to cell cultures affected the activation state of Akt and GSK3β, levels of phospho-Ser473 Akt and phospho-Ser9 GSK3β were determined in homogenates of SH-SY5Y cells preincubated with 5 μM ADDL. Western blots (Fig. 7) showed that ADDLs reduced pSer473-Akt, with the consequent reduced kinase activity of this protein, and also reduced the amount of its downstream target pSer9-GSK3β, which would result in an increase in GSK3β kinase activity.

Data obtained with amyloidogenic AD animal models and cultured neural cells indicate that Aβ may be responsible of an Akt- and GSK3β-mediated increase in phospho-VDAC1, more prone than the dephosphorylated form to induce the release of pro-apoptotic factors [29].

DISCUSSION

Mitochondria are key players in apoptotic processes underlying neuronal death in neurodegenerative diseases. VDAC, as mitochondrial porin also found in the neuronal membrane (pl-VDAC), is related to redox homeostasis and apoptosis. Structure of mitochondria and expression of mitochondrial proteins is altered in AD [30]. Whether mitochondrial alterations are the result of impaired turnover and removal of damaged mitochondria, or damaged mitochondria at the dystrophic neurites are the consequence of altered expression and function of mitochondrial proteins is not known. We here report an increase in VDAC1 protein expression in transgenic mice expressing high levels of Aβ and also in postmortem brain tissue from AD patients at an advanced stage of the disease. Addition of Aβ oligomers (ADDLs) to cell cultures increased VDAC1 levels supporting a role of Aβ in VDAC1 expression. Aβ also appears to promote phosphorylation of VDAC1, which would subsequently facilitate the leakage of mitochondrial proapoptotic molecules, suggesting a contribution of VDAC1 to the neurotoxic effects of Aβ.

Although the exact cause of AD is still a matter of considerable debate [31], the amyloid cascade hypothesis has provided a useful framework for the research on this neurodegenerative disease for nearly 20 years [27]. Accordingly, an increased production or decreased clearance of Aβ peptide would be one of the main causes of the disease. To confirm this hypothesis transgenic mouse producing high levels of Aβ are a suitable model. In the present report, it is shown that VDAC1 protein levels increased in the hippocampus of Tg2576 mice, the increase being apparently related to Aβ production. The increase in VDAC1 levels was already evident at the age of 7 months, when Aβ also starts to be significantly produced [8]. Reinforcing the argument, J20 mice, another transgenic line with higher Aβ brain levels than Tg2576 mice [16], displayed a significant elevation of VDAC in hippocampal homogenates from 7 month-old animals (see Fig. 2B), thus supporting a causal link for Aβ on VDAC increase in AD mice models. It should be noted that the results of Western-blot studies were confirmed by immunohistochemical analysis showing that both Tg2576 and J20 mice displayed a marked rise in VDAC1 immunoreactivity in the CA1 subfield of the hippocampus, a brain region that is known to be selectively vulnerable in human AD brains. High levels of VDAC were also found in postmortem brain samples from AD patients thus confirming that the finding was not restricted to animal models.

ADDLs are soluble Aβ oligomers whose *in vivo* administration more strongly correlates with memory impairment than that of monomeric forms [32]. In Tg2576 mice, spatial memory impairment coincides with the appearance of Aβ soluble oligomers leading to the hypothesis that Aβ oligomers are more toxic than

the monomer [7, 32]. These nonfibrillar assemblies of Aβ have been found also in brain extracts from AD patients [33]. Oligomer toxicity may be related to alterations in the Akt/GSK3β cascade and in fact ADDLs promoted VDAC1 overexpression in neuroblastoma cell cultures which was paralleled with a decrease of Akt activity and with an increase in GSK3β activity. VDAC1 possesses a GSK3β phosphorylation consensus motif at amino acids 51 to 55. Mutation of VDAC Thr51 prevents the ability of GSK3β to phosphorylate it [14]. The kinase Akt regulates GSK3β activity by phosphorylation at Ser9. Accordingly, we found decreased levels of active Akt (pSer473-Akt) and also decreased levels of inactive GSK3β (pSer9-GSK3β) in the hippocampus of AD mice models. Overall, it seems that phosphorylation of VDAC1 in hippocampal neurons could be, at least in part, performed by GSK3β.

In the hippocampus of transgenic mice, phosphorylated VDAC1 was the predominant form. Phosphorylation of the protein prevents its interaction with anti-apoptotic proteins, such as HXK, and favors the release of pro-apoptotic factors. VDAC1 is supposed to be an essential player in apoptosis [34]. Overexpression of human and murine VDAC1 induces apoptotic cell death, regardless of the cell type [35–37]. There are two possible mechanisms underlying VDAC1 role in apoptosis. According to the first one, VDAC1 overexpression stimulates its oligomerization facilitating the release of mitochondrial apoptogenic proteins such as cytochrome c, the activator of caspases Smac/Diablo or the apoptosis-inducing factor (AIF) [38]. The second mechanism is related with its interaction with HXK since the interaction favors a close state, whereas the release of HXK promotes an open state that is more prone to the release of mitochondrial pro-apoptotic factors. VDAC1 function in mitochondrial transport is regulated via interaction with associated proteins such as members of the Bcl2 family and HXK. Strong evidence supports VDAC-HXK interaction [35, 37, 39] and the effect of this interaction on apoptosis (reviewed in [34]). Conformational changes due to phosphorylation of VDAC1 is one of the mechanisms that provoke the disruption of the VDAC-HXK interaction in mitochondria [14]. In fact, when VDAC1 is phosphorylated on the putative GSK3β epitope, i.e., Thr51, HXK is unable to interact with VDAC1, thus dissociating from the mitochondria. In the present report, it was shown that the hippocampus from 12 month-old Tg2576 mice had increased levels of pThr-VDAC1 coincident with lower HXK levels. Targeted disruption of mitochondria-HXK interaction or exposure to proapoptotic stimuli that promote rapid dissociation of HXK from mitochondria potently induce cytochrome c release and apoptosis [29].

Taken together, our results indicate that VDAC1 overexpression could make hippocampal neurons more sensitive to death. One of the major consequences of GSK3β activation in AD is the hyperphosphorylation of the tau protein, which leads to cytoskeletal destabilization and synapse dysfunction. Our data also implicate this kinase in the neurodegenerative cascade through the disruption of HXK-VDAC interaction by VDAC1 phosphorylation. As apoptotic cell death has been shown to represent the terminal process in some neurodegenerative diseases such as AD, agents that maintain the homeostasis of VDAC1 may offer new and effective means of treating the disease. Modulation of VDAC1 activity and/or phosphorylation may therefore be considered as a potential therapeutic target addressed at reducing the release of mitochondrial proapoptotic factors that impact into the viability of hippocampal neurons.

ACKNOWLEDGMENTS

This study was supported by Grants from the Department of Education of the Government of Navarra, Spanish Ministry of Health (CIBERNED), Ministry of Science and Innovation (SAF 2008-02342) and UTE project FIMA, Spain. We thank Susana Ursúa, María Espelosín, and Esther Gimeno and the animal facility of CIMA for technical support and Dr. Rafael Franco for critical review of this manuscript. The authors declare that, except for income received from the primary employer, no financial support or compensation has been received from any individual or corporate entity over the past 3 years for research or professional service and there are no personal financial holdings that could be perceived as constituting a potential conflict of interest.

Authors' disclosures available online (http://www.j-alz.com/disclosures/view.php?id=621).

REFERENCES

[1] Selkoe DJ (1999) Translating cell biology into therapeutic advances in Alzheimer's disease. *Nature* **399**, A23-A31.
[2] Hardy J, Selkoe DJ (2002) The amyloid hypothesis of Alzheimer's disease: progress and problems on the road to therapeutics. *Science* **297**, 353-356.
[3] Selkoe DJ (1997) Alzheimer's disease: genotypes, phenotypes, and treatments. *Science* **275**, 630-631.
[4] Howlett DR, Richardson JC (2009) The pathology of APP transgenic mice: a model of Alzheimer's disease or sim-

ply overexpression of APP? *Histol Histopathol* **24**, 83-100.

[5] Chapman PF, White GL, Jones MW, Cooper-Blacketer D, Marshall VJ, Irizarry M, Younkin L, Good MA, Bliss TV, Hyman BT, Younkin SG, Hsiao KK (1999) Impaired synaptic plasticity and learning in aged amyloid precursor protein transgenic mice. *Nat Neurosci* **2**, 271-276.

[6] Hsiao K, Chapman P, Nilsen S, Eckman C, Harigaya Y, Younkin S, Yang F, Cole G (1996) Correlative memory deficits, Abeta elevation, and amyloid plaques in transgenic mice. *Science* **274**, 99-102.

[7] Westerman MA, Cooper-Blacketer D, Mariash A, Kotilinek L, Kawarabayashi T, Younkin LH, Carlson GA, Younkin SG, Ashe KH (2002) The relationship between Abeta and memory in the Tg2576 mouse model of Alzheimer's disease. *J Neurosci* **22**, 1858-1867.

[8] Kawarabayashi T, Younkin LH, Saido TC, Shoji M, Ashe KH, Younkin SG (2001) Age-dependent changes in brain, CSF, and plasma amyloid (beta) protein in the Tg2576 transgenic mouse model of Alzheimer's disease. *J Neurosci* **21**, 372-381.

[9] Morgan D, Diamond DM, Gottschall PE, Ugen KE, Dickey C, Hardy J, Duff K, Jantzen P, DiCarlo G, Wilcock D, Connor K, Hatcher J, Hope C, Gordon M, Arendash GW (2000) A beta peptide vaccination prevents memory loss in an animal model of Alzheimer's disease. *Nature* **408**, 982-985.

[10] Ferrer I (2009) Altered mitochondria, energy metabolism, voltage-dependent anion channel, and lipid rafts converge to exhaust neurons in Alzheimer's disease. *J Bioenerg Biomembr* **41**, 425-431.

[11] Devi L, Prabhu BM, Galati DF, Avadhani NG, Anandatheerthavarada HK (2006) Accumulation of amyloid precursor protein in the mitochondrial import channels of human Alzheimer's disease brain is associated with mitochondrial dysfunction. *J Neurosci* **26**, 9057-9068.

[12] Wang X, Su B, Lee HG, Li X, Perry G, Smith MA, Zhu X (2009) Impaired balance of mitochondrial fission and fusion in Alzheimer's disease. *J Neurosci* **29**, 9090-9103.

[13] Sampson MJ, Lovell RS, Craigen WJ (1997) The murine voltage-dependent anion channel gene family. Conserved structure and function. *J Biol Chem* **272**, 18966-18973.

[14] Pastorino JG, Hoek JB, Shulga N (2005) Activation of glycogen synthase kinase 3beta disrupts the binding of hexokinase II to mitochondria by phosphorylating voltage-dependent anion channel and potentiates chemotherapy-induced cytotoxicity. *Cancer Res* **65**, 10545-10554.

[15] Perez-Gracia E, Torrejon-Escribano B, Ferrer I (2008) Dystrophic neurites of senile plaques in Alzheimer's disease are deficient in cytochrome c oxidase. *Acta Neuropathol* **116**, 261-268.

[16] Mucke L, Masliah E, Yu GQ, Mallory M, Rockenstein EM, Tatsuno G, Hu K, Kholodenko D, Johnson-Wood K, McConlogue L (2000) High-level neuronal expression of abeta$_{1-42}$ in wild-type human amyloid protein precursor transgenic mice: synaptotoxicity without plaque formation. *J Neurosci* **20**, 4050-4058.

[17] Klein WL (2002) A[beta] toxicity in Alzheimer's disease: globular oligomers (ADDLs) as new vaccine and drug targets. *Neurochem Int* **41**, 345-352.

[18] Biedler JL, Roffler-Tarlov S, Schachner M, Freedman LS (1978) Multiple neurotransmitter synthesis by human neuroblastoma cell lines and clones. *Cancer Res* **38**, 3751-3757.

[19] Hope T, Keene J, Gedling K, Cooper S, Fairburn C, Jacoby R (1997) Behaviour changes in dementia. 1: Point of entry data of a prospective study. *Int J Geriatr Psychiatry* **12**, 1062-1073.

[20] Roth M, Tym E, Mountjoy CQ, Huppert FA, Hendrie H, Verma S, Goddard R (1986) CAMDEX. A standardised instrument for the diagnosis of mental disorder in the elderly with special reference to the early detection of dementia. *Br J Psychiatry* **149**, 698-709.

[21] American Psychiatric Association (1987) *Diagnostic and Statistical Manual of Mental Disorders*, American Psychiatric Press, Washington, DC.

[22] McKhann G, Drachman D, Folstein M, Katzman R, Price D, Stadlan EM (1984) Clinical diagnosis of Alzheimer's disease: report of the NINCDS-ADRDA Work Group under the auspices of Department of Health and Human Services Task Force on Alzheimer's Disease. *Neurology* **34**, 939-944.

[23] Folstein MF, Folstein SE, McHugh PR (1975) "Mini-mental state." A practical method for grading the cognitive state of patients for the clinician. *J Psychiatr Res* **12**, 189-198.

[24] Mirra SS, Heyman A, McKeel D, Sumi SM, Crain BJ, Brownlee LM, Vogel FS, Hughes JP, van Belle G, Berg L (1991) The Consortium to Establish a Registry for Alzheimer's Disease (CERAD). Part II. Standardization of the neuropathologic assessment of Alzheimer's disease. *Neurology* **41**, 479-486.

[25] Simon AM, Schiapparelli L, Salazar-Colocho P, Cuadrado-Tejedor M, Escribano L, Lopez de Maturana R, Del Rio J, Perez-Mediavilla A, Frechilla D (2009) Overexpression of wild-type human APP in mice causes cognitive deficits and pathological features unrelated to Abeta levels. *Neurobiol Dis* **33**, 369-378.

[26] Braak H, Braak E (1998) Evolution of neuronal changes in the course of Alzheimer's disease. *J Neural Transm Suppl* **53**, 127-140.

[27] Hardy JA, Higgins GA (1992) Alzheimer's disease: the amyloid cascade hypothesis. *Science* **256**, 184-185.

[28] Lambert MP, Barlow AK, Chromy BA, Edwards C, Freed R, Liosatos M, Morgan TE, Rozovsky I, Trommer B, Viola KL, Wals P, Zhang C, Finch CE, Krafft GA, Klein WL (1998) Diffusible, nonfibrillar ligands derived from Abeta$_{1-42}$ are potent central nervous system neurotoxins. *Proc Natl Acad Sci U S A* **95**, 6448-6453.

[29] Majewski N, Nogueira V, Bhaskar P, Coy PE, Skeen JE, Gottlob K, Chandel NS, Thompson CB, Robey RB, Hay N (2004) Hexokinase-mitochondria interaction mediated by akt Is Required to inhibit apoptosis in the presence or absence of bax and bak. *Mol Cell* **16**, 819-830.

[30] Ramirez CM, Gonzalez M, Diaz M, Alonso R, Ferrer I, Santpere G, Puig B, Meyer G, Marin R (2009) VDAC and ERalpha interaction in caveolae from human cortex is altered in Alzheimer's disease. *Mol Cell Neurosci* **42**, 172-183.

[31] Pimplikar SW (2009) Reassessing the amyloid cascade hypothesis of Alzheimer's disease. *Int J Biochem Cell Biol* **41**, 1261-1268.

[32] Lesne S, Koh MT, Kotilinek L, Kayed R, Glabe CG, Yang A, Gallagher M, Ashe KH (2006) A specific amyloid-beta protein assembly in the brain impairs memory. *Nature* **440**, 352-357.

[33] Gong Y, Chang L, Viola KL, Lacor PN, Lambert MP, Finch CE, Krafft GA, Klein WL (2003) Alzheimer's disease-affected brain: presence of oligomeric A beta ligands (ADDLs) suggests a molecular basis for reversible memory loss. *Proc Natl Acad Sci U S A* **100**, 10417-10422.

[34] Shoshan-Barmatz V, Keinan N, Zaid H (2008) Uncovering the role of VDAC in the regulation of cell life and death. *J Bioenerg Biomembr* **40**, 183-191.

[35] Abu-Hamad S, Zaid H, Israelson A, Nahon E, Shoshan-Barmatz V (2008) Hexokinase-I protection against apoptotic cell death is mediated via interaction with the voltage-dependent anion channel-1: mapping the site of binding. *J Biol Chem* **283**, 13482-13490.

[36] Ghosh T, Pandey N, Maitra A, Brahmachari SK, Pillai B (2007) A role for voltage-dependent anion channel VDAC1 in polyglutamine-mediated neuronal cell death. *PLoS One* **2**, e1170.

[37] Zaid H, Abu-Hamad S, Israelson A, Nathan I, Shoshan-Barmatz V (2005) The voltage-dependent anion channel-1 modulates apoptotic cell death. *Cell Death Differ* **12**, 751-760.

[38] Shoshan-Barmatz V, Keinan N, Abu-Hamad S, Tyomkin D, Aram L Apoptosis is regulated by the VDAC1 N-terminal region and by VDAC oligomerization: release of cytochrome c, AIF and Smac/Diablo. *Biochim Biophys Acta* **1797**, 1281-1291.

[39] Pastorino JG, Hoek JB (2003) Hexokinase II: the integration of energy metabolism and control of apoptosis. *Curr Med Chem* **10**, 1535-1551.